Version of Record at: https://doi.org/10.1029/2023GL105363

Check for updates

AGU ADVANCING EARTH AND SPACE SCIENCES

Geophysical Research Letters

RESEARCH LETTER
10.1029/2023GL105363

Impact of Marine Heatwaves on Air-Sea CO_2 Flux Along the US East Coast

Kelsea Edwing[1], Zelun Wu[1,2,3,4], Wenfang Lu[5,6], Xinyu Li[1], Wei-Jun Cai[1], and Xiao-Hai Yan[1,3]

[1]School of Marine Science and Policy, University of Delaware, Newark, DE, USA, [2]College of Ocean and Earth Science, Xiamen University, Xiamen, China, [3]Joint Institute for Coastal Research and Management (Joint-CRM), University of Delaware, Newark, DE, USA, [4]State Key Laboratory of Marine Environmental Science, Xiamen University, Xiamen, China, [5]School of Marine Sciences, Sun Yat-Sen University, Zhuhai, China, [6]Southern Marine Science and Engineering Guangdong Laboratory (Zhuhai), Zhuhai, China

Key Points:

- Marine heatwaves (MHWs) primarily generated positive sea surface pCO_2 (pCO_{2sea}) anomalies in the Mid-Atlantic Bight (MAB) and South Atlantic Bight (SAB) but had a larger impact on air-sea CO_2 flux anomalies in the MAB
- Reduced wind speeds amplified MHW contributions during CO_2 sink months and counteracted them during CO_2 source months
- In the MAB, wintertime atmospheric perturbations related to zonal shifts in the jet stream produce slower wind speeds which aid in generating air-sea heat flux type MHW events that ultimately reduce oceanic CO_2 uptake

Supporting Information:

Supporting Information may be found in the online version of this article.

Correspondence to:

Z. Wu and X.-H. Yan,
zelunwu@outlook.com;
xiaohai@udel.edu

Citation:

Edwing, K., Wu, Z., Lu, W., Li, X., Cai, W.-J., & Yan, X.-H. (2024). Impact of marine heatwaves on air-sea CO_2 flux along the US East Coast. *Geophysical Research Letters*, *51*, e2023GL105363. https://doi.org/10.1029/2023GL105363

Received 6 JUL 2023
Accepted 8 DEC 2023

Author Contributions:

Conceptualization: Zelun Wu
Formal analysis: Kelsea Edwing
Funding acquisition: Xiao-Hai Yan
Methodology: Kelsea Edwing, Zelun Wu
Project Administration: Xiao-Hai Yan
Supervision: Xiao-Hai Yan
Validation: Zelun Wu
Visualization: Kelsea Edwing
Writing – original draft: Kelsea Edwing

Abstract Marine heatwaves (MHWs) are extremely warm ocean temperature events that significantly affect marine environments, but their effects on the coastal carbonate system are still uncertain. In this study, we systematically quantify MHWs' impacts on air-sea carbon dioxide (CO_2) flux anomalies (FCO_2') in the Mid-Atlantic Bight (MAB) and South Atlantic Bight (SAB) from 1992 to 2020. During the longest MHW in both regions, oceanic CO_2 uptake capabilities substantially decreased, primarily due to significant increases in the seawater partial pressure of CO_2 (pCO_{2sea}). For all cases, MHWs played a more significant role in driving pCO_{2sea} changes in the MAB than the SAB, where non-thermal drivers dominated pCO_{2sea} variability. In the MAB, weakened wind speeds related to wintertime atmospheric perturbations increase ocean temperatures and pCO_{2sea}, further reducing CO_2 uptake during winter MHWs. This work is the first to connect extreme temperatures to coastal air-sea CO_2 fluxes. The reduction in CO_2 absorption noted during MHWs in this study has important implications for coastal regions to act as continued sinks for excess CO_2 emissions in the atmosphere.

Plain Language Summary The transfer of carbon dioxide (CO_2) between the atmosphere and ocean is sensitive to sea surface temperature (SST) changes because warmer SSTs increase the sea surface partial pressure of CO_2 and reduce the ocean's ability to absorb CO_2 from the atmosphere. It is, therefore, conceivable that marine heatwaves (MHWs), which are extremely warm ocean temperature events, could modify how carbon moves between the ocean and the atmosphere. This study provides the first attempt to evaluate the impacts of MHWs on the air-sea CO_2 flux (FCO_2) anomalies along the US East Coast, encompassing the Mid-Atlantic Bight (MAB) and South Atlantic Bight (SAB) during 1992–2020. Both regions experienced reduced CO_2 absorption in response to the longest MHWs in each region. These extreme temperatures had a larger impact on CO_2 absorption in the MAB compared to the SAB, where non-temperature factors were more influential. The coastal ocean plays an important role in helping to mitigate human-induced climate change by absorbing excess CO_2 from the atmosphere. As such, the demonstrated reduced absorption of the ocean associated with MHWs in this study, which might also apply to other coastal locations, has vital implications for the efficiency of the ocean in offsetting global warming impacts.

1. Introduction

Anthropogenic climate change exhibits extensive effects on the global climate system, notably resulting in rising air and sea surface temperatures (Dye et al., 2013; Large & Yeaher, 2012; Salinger et al., 2005; Seager et al., 2019) and increasing the prevalence of extreme events (Elsner, 2006; Jentsch et al., 2007; Sillmann & Roeckner, 2007; Stott, 2016). The ocean is currently estimated as a net sink for atmospheric carbon dioxide (CO_2) (Friedlingstein et al., 2022; Laruelle et al., 2018; Le Quéré et al., 2010), leading to fundamental shifts in Earth's climate system by absorbing approximately 25% of anthropogenic carbon emissions since the preindustrial era (Friedlingstein et al., 2022). However, CO_2 uptake could be weakened due to the prevalence of extreme events, such as marine heatwaves (MHWs, Hobday et al., 2018; Mignot et al., 2022). MHWs are prolonged, anomalously warm seawater events that can persist for days to months and range in size up a thousand kilometers or more (Frölicher et al., 2018; Hobday et al., 2016; Scannell et al., 2016). They have increased in frequency, intensity, and duration over the past two centuries (Oliver et al., 2018), and occur frequently in the eastern continental margins

Writing – review & editing: Kelsea Edwing, Zelun Wu, Wenfang Lu, Xinyu Li, Wei-Jun Cai, Xiao-Hai Yan

of the United States (Chen et al., 2014, 2015; Gawarkiewicz et al., 2019). However, their influence on carbonate system parameters like seawater partial pressure of CO_2 (pCO_{2sea}) and, therefore, air-sea CO_2 flux in this region remains insufficiently investigated.

Air-sea CO_2 flux (FCO_2) quantifies the exchange of CO_2 between the atmosphere and ocean. The difference between seawater (pCO_{2sea}) and the atmospheric partial pressure of CO_2 (pCO_{2air}), ΔpCO_2, determines whether the ocean is taking up CO_2 from the atmosphere (negative ΔpCO_2) or emitting CO_2 to the atmosphere (positive ΔpCO_2). Spatial and temporal variations in pCO_{2air} are small, so ΔpCO_2 variability is primarily controlled by variations in pCO_{2sea} (Sarmiento & Gruber, 2006). Spatiotemporal pCO_{2sea} changes are driven by thermodynamics, mixing, biological activities, and air-sea gas exchange. Since MHW events are extremely warm SST events, it is conceivable that MHWs could impact pCO_{2sea} and therefore FCO_2 via thermodynamics.

Despite this, literature connecting MHWs and FCO_2 is limited. One study found that prolonged MHWs reduced CO_2 uptake in major North Pacific open-ocean uptake regions and, due to linkages with the El Nino Southern Oscillation (ENSO), reduced CO_2 release in major tropical Pacific open-ocean outgassing areas (Mignot et al., 2022). However, the influence of MHWs on nearshore carbonate systems in continental shelves needs to be better understood. Despite the coastal ocean constituting only 7%–10% of the world's oceans, it is argued to play a disproportionately large role in the uptake of CO_2 by the ocean (Dai et al., 2022; Gattuso et al., 1998; Le Quéré et al., 2009, 2010; Liu et al., 2010; Najjar et al., 2012). Therefore, understanding how coastal air-sea CO_2 fluxes are potentially modulated by MHW events is not only important for furthering our comprehension of coastal biogeochemical cycles, but also for improving climate models and predictions of future climate change impacts.

This study focuses on the Mid-Atlantic Bight (MAB, Figure 1a) and South Atlantic Bight (SAB, Figure 1b), two regions on the U.S. East Coast that are well-studied and have decades of inorganic carbonate data available (e.g., Cai et al., 2020; Li et al., 2022). Though regional differences in physical and biological processes exist, both the MAB and SAB have been consistently estimated as net sinks of atmospheric CO_2, with the MAB's CO_2 flux density estimated as -0.73 to -1.90 mol C m^{-2} yr^{-1} (Cahill et al., 2016; DeGrandpre et al., 2002; Fennel et al., 2008; Laruelle et al., 2018; Signorini et al., 2013), and the SAB's as -0.48 to -0.75 mol C m^{-2} yr^{-1} (Cahill et al., 2016; Jiang et al., 2008; Signorini et al., 2013). Cai et al. (2020) found that pCO_{2sea} variations along the US East Coast reflect local, short-term modifications by coastal physical and biological processes. Under extreme cases like MHW events, pCO_{2sea} and, therefore, FCO_2, may be more sensitive to significant increases in SST and potentially switch coastal CO_2 sinks to sources for the atmosphere. As such, this study aims to quantify the changes in pCO_{2sea} and FCO_2 during MHWs in the MAB and SAB and understand the underlying dynamics. To achieve this goal, we first examined each region's most prolonged MHW event from 1992 to 2020. We then investigated the common patterns and mechanisms underlying changes in pCO_{2sea} and FCO_2 during MHWs in each region to identify the conditions under which CO_2 flux will substantially change. The following section describes the data and methods used for MHW detection and FCO_2 calculations. Section 3 presents and discusses the results, and Section 4 reiterates the conclusions.

2. Data and Methods

2.1. Marine Heatwave Detection

We utilized the Daily Optimum Interpolation Sea Surface Temperature v2 (OISST) data set from the National Oceanic and Atmospheric Administration (NOAA) (Reynolds et al., 2002) to detect MHWs within the period 1992/01–2020/12. OISST has a spatial resolution of 0.25° × 0.25°. The MAB and SAB regions (depth < 200 m) were analyzed separately using this daily gridded data. The MAB is composed of 193 grid cells, spanning from Cape Hatteras, North Carolina (35° north) to Cape Cod, Massachusetts (41.5°N), while the SAB consists of 163 grid cells ranging between Cape Canaveral, Florida (26°N) to Cape Hatteras, North Carolina (35°N).

Using the daily gridded SSTs, MHWs were detected in each grid cell following the definition from Hobday et al. (2016), that is, the period that SSTs are above the 90th percentile threshold of the climatology. For this study, the climatology was computed from 1992 to 2020. The CO_2 data used in this study is limited to monthly resolution, so we cannot determine the impact of individual MHW events by day. Instead, we examine the influence of MHW months. The number of days a MHW was detected in each grid was summed for each month (348 in total) within the 28-year study period. Individual months with 15 or more MHW days are considered MHW months because we expect that the impact of extreme temperatures that endure for at least half a month should be reflected in the pCO_2 and CO_2 flux data. The remaining months are defined as non-MHW months.

AGU ADVANCING EARTH AND SPACE SCIENCES

Geophysical Research Letters

10.1029/2023GL105363

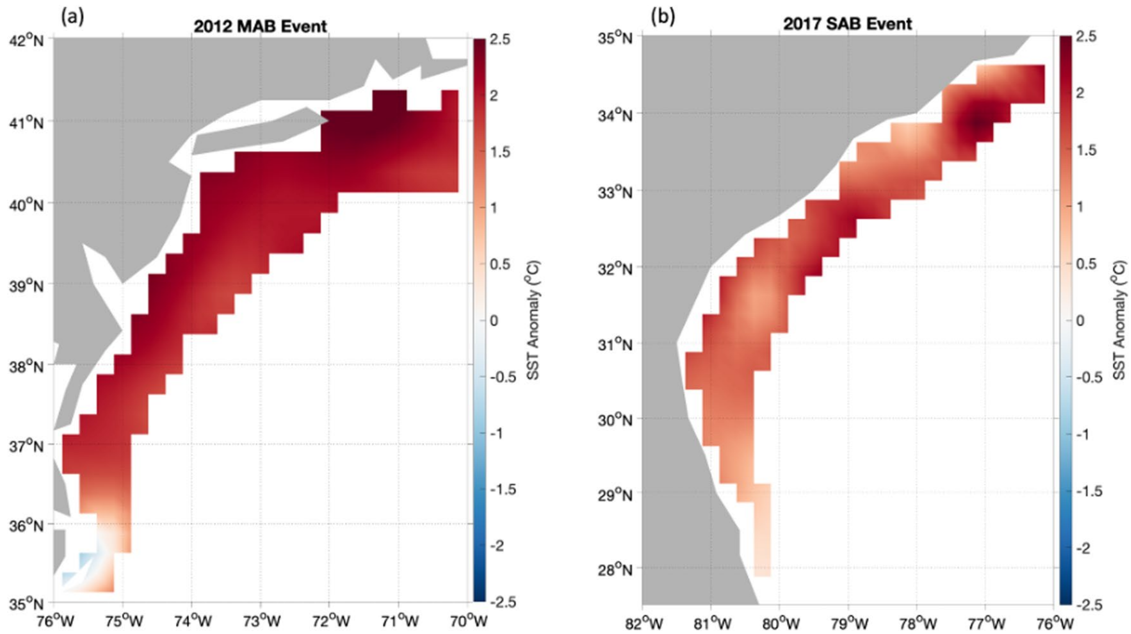

Figure 1. Average monthly sea surface temperature anomalies during (a) the 2012 MAB event from February 2012 to June 2012 and (b) the 2017 SAB event in April 2017.

2.2. Air-Sea CO_2 Flux Calculation

Monthly air-sea CO_2 flux (FCO_2) from January 1992 to December 2020 was calculated using the gas exchange formula (Wanninkhof et al., 2009),

$$FCO_2 = k\,K_0(pCO_{2sea} - pCO_{2air}) \tag{1}$$

where k is the gas transfer velocity, K_0 is CO_2 solubility in seawater, pCO_{2sea} and pCO_{2air} are the partial pressure of CO_2 in the ocean and atmosphere, respectively. A positive or negative FCO_2 value indicates the ocean is acting as a CO_2 source or sink to the atmosphere. Gas transfer velocity (k) is calculated using wind speed at 10-m (U_{10}) above the sea surface (Wanninkhof, 2014),

$$k = 0.251{U_{10}}^2(\mathrm{Sc}/660)^{-0.5} \tag{2}$$

where U_{10} is monthly 10-m wind speeds from the fifth generation ECMWF high-resolution global reanalysis data set, ERA5 (Hersbach et al., 2023), which contains monthly gridded atmospheric data at 0.25° × 0.25° resolution from 1959 to present. Sc is the Schmidt number and is specific to CO_2 (Wanninkhof, 2014),

$$\mathrm{Sc} = 2116.8 - 136.25(\mathrm{SST}) + 4.7353(\mathrm{SST})^2 - 0.092307(\mathrm{SST})^3 + 0.0007555(\mathrm{SST})^4 \tag{3}$$

In situ SST, SSS, and sea surface fCO_2 were obtained from the gridded Surface Ocean CO_2 Atlas (SOCAT) version 2022 (0.25° × 0.25°). fCO_2 was converted to sea surface pCO_2 (Takahashi et al., 2019). Atmospheric CO_2 mole fractions in dry air (xCO_{2air}; in ppm) were downloaded from NOAA's zonally averaged Greenhouse Gas Marine Boundary Layer Reference (MBL Reference, Conway et al., 1994). The MBL reference is composed of weekly air samples collected at a subset of sites globally from NOAA's Cooperative Air Sampling Network and has a spatial resolution of 0.05 sine of the latitude. Monthly air samples were obtained by averaging all weekly values for each month. pCO_{2air} was calculated from xCO_{2air} using the conversion equation (Sarmiento & Gruber, 2006):

$$pCO_{2air} = xCO_{2air}(1 - p_w) \tag{4}$$

where p_w is the water vapor pressure, which is assumed to be at saturation in the vicinity of the air-sea interface (Weiss & Price, 1980):

$$p_w = \exp[24.4543 - 67.4509(100/\mathrm{SST}) - 4.8489(100/\mathrm{SST}) - 0.000544(\mathrm{SSS})] \tag{5}$$

CO_2 solubility (K_0) is a function of absolute SST and SSS (Weiss, 1974):

$$\ln(K_0) = A_1 + A_2\left(\frac{100}{\text{SST}}\right) + A_3 \ln\left(\frac{\text{SST}}{100}\right) + \text{SSS}\left[B_1 + B_2\left(\frac{\text{SST}}{100}\right) + B_3\left(\frac{\text{SST}}{100}\right)^2\right] \quad (6)$$

where $A_1 = -58.0931$, $A_2 = 90.5069$, $A_3 = 22.2940$, $B_1 = 0.027766$, $B_2 = -0.025888$, and $B_3 = 0.0050578$ are CO_2-specific coefficients. The SOCAT database is comprised of in situ observations, which means data gaps are present. Months without data were excluded from analysis.

2.3. Thermal and Non-Thermal Components of pCO_{2sea} Anomalies

Since pCO_{2sea} is the dominant factor influencing CO_2 flux, changes (i.e., anomalies) in this parameter would likely induce CO_2 flux anomalies. To isolate the influence of SSTs (i.e., MHWs) on pCO_{2sea} anomalies (denoted using a prime, pCO_{2sea}'), we calculate the thermal ($pCO_2{}'_T$) and non-thermal components ($pCO_2{}'_{NT}$) of pCO_{2sea}',

$$p\text{CO}_2{}'_T = \overline{p\text{CO}_2} * \exp\left(0.0423\left(\text{SST} - \overline{\text{SST}}\right)\right) - \overline{pCO_2} \quad (7)$$

$$p\text{CO}_2{}'_{\text{NT}} = p\text{CO}_2 * \exp\left(0.0423\left(\overline{\text{SST}} - \text{SST}\right)\right) - \overline{pCO_2} \quad (8)$$

where $\overline{p\text{CO}_2}$ and $\overline{\text{SST}}$ are the monthly pCO_{2sea} and SST climatology, respectively. The temperature sensitivity of pCO_{2sea} is set as $0.0423°\text{C}^{-1}$ (Takahashi et al., 1993, 2002). The thermal component represents the pCO_{2sea}' driven by SST change and the non-thermal component represents pCO_{2sea}' driven by other non-temperature factors, including dissolved inorganic carbon (DIC), total alkalinity (TA), and SSS change. Processes effecting non-thermal parameters include biological activities (Cao et al., 2020; Signorini et al., 2013), physical transport and mixing (Cao et al., 2020; Jiang et al., 2008, 2013), and air-sea gas exchange (Cai et al., 2020; Xu et al., 2020). In this work, a student's *t*-test is used to test whether anomalies are significantly different from zero at a 95% confidence interval (i.e., statistically signifigant at *p*-value of 0.05 or 5%).

2.4. Taylor Expansion of Air-Sea CO_2 Flux

SST is positively correlated with gas transfer velocity (k) and negatively correlated with CO_2 solubility (K_0). As a result, the variability of the gas transfer coefficient (Γ), the product of k and K_0, is almost independent of SST and is instead predominately controlled by wind speed (Wanninkhof & Triñanes, 2017). To understand which factor (ΔpCO_2 or wind) is driving FCO_2 anomalies during marine heatwave and non-marine heatwave months, a Reynolds decomposition of the CO_2 flux anomaly (FCO_2') is computed. This expansion reveals the relative contributions of the two flux components (i.e., ΔpCO_2 and Γ) in the MAB and SAB. Each flux component (example: ΔpCO_2) is considered the sum of their long-term monthly mean (i.e., climatology; $\overline{\Delta p\text{CO}_2}$) and anomaly ($\Delta pCO_2'$). Thus, the decomposition of FCO_2 begins as:

$$\text{FCO}_2 = \left(\overline{\Gamma} + \Gamma'\right)\left(\overline{\Delta p\text{CO}_2} + \Delta p\text{CO}_2{}'\right) \quad (9)$$

Rearrangement of Equation 9 into their zero, first, second, and higher order terms produces:

$$\text{FCO}_2 = \overline{\Gamma\Delta p\text{CO}_2} + \left(\overline{\Gamma}\right)\left(\Delta p\text{CO}_2{}'\right) + \left(\overline{\Delta pCO_2}\right)\left(\Gamma'\right) + \Gamma'\Delta p\text{CO}_2{}' \quad (10)$$

where the first term on the right-hand side is the zero-order term (i.e., the FCO_2 climatology), the next two terms are the first-order terms, and the last term is the second-order term. Since CO_2 flux anomaly (FCO_2') is the focus of this analysis, Equation 10 can be consolidated into:

$$\text{FCO}_2{}' = \left(\overline{\Gamma}\right)\left(\Delta p\text{CO}_2{}'\right) + \left(\overline{\Delta p\text{CO}_2}\right)\left(\Gamma'\right) + (\text{O}_2) \quad (11)$$

where the terms on the right-hand side of Equation 11 represent the contribution to FCO_2' from oceanic and atmospheric pCO_2 anomalies (housed within the ΔpCO_2 term) and wind speed anomalies (housed within the gas transfer coefficient, Γ), and (O_2) is the higher-order residual term that can be neglected. The component with the largest contribution is the dominant term driving the FCO_2 anomalies during each month in the MAB and SAB.

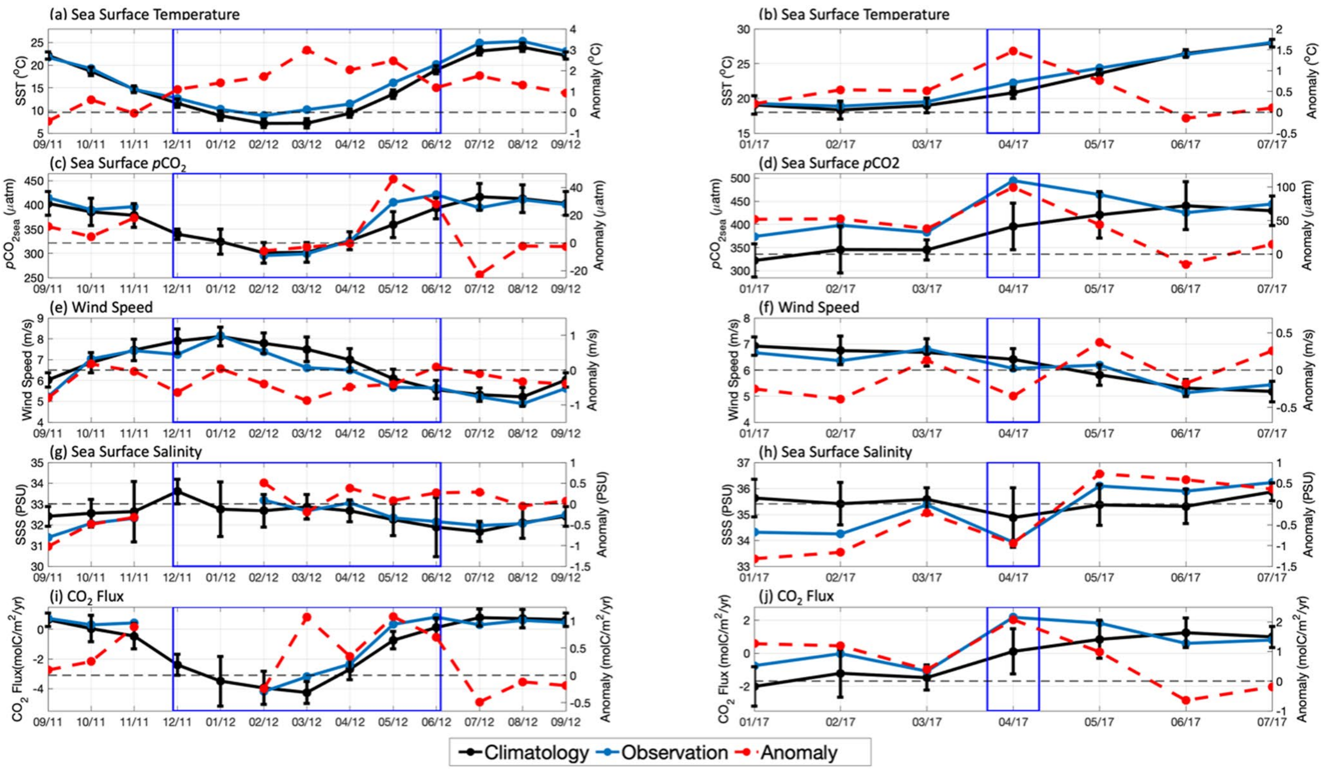

Figure 2. Monthly values (blue), climatology (black), and anomalies (red) of (a and b) SST, (c and d) sea surface pCO_2, (e and f) wind speed, (g and h) SSS, and (i and j) FCO_2 during the 2012 MAB event (left panels) and the 2017 SAB event (right panels). Blue squares in each plot highlight the 2012 and 2017 MHW events in the MAB (left) and SAB (right). Black error bars are one standard deviation associated with the monthly climatology in each panel.

3. Results and Discussion

3.1. Case Studies: Two Most Prolonged MHW Events in the MAB and SAB

To investigate the response of sea surface pCO_{2sea} and CO_2 flux to MHWs, we begin by examining the two most prolonged MHWs in the MAB and SAB, respectively. These two events provide a valuable opportunity to examine changes in pCO_2 and FCO_2 in response to the longest exposure period of the sea surface to extreme temperatures. Insights from these two case study events may be generally representative of the impact of all prolonged MHWs on pCO_2 and FCO_2. The longest event in the MAB lasted over 200 days (25 November 2011–15 June 2012), named the "2012 MAB event." Analysis focused on the overlapping period between the MHW event and available SOCAT observations from February 2012 to June 2012 (5 months, Figure 1a). The longest MHW event in the SAB, referred to as the "2017 SAB event," lasted for 44 days (21 March 2017–05 May 2017). To maintain the definition of a MHW month, analysis focused on April 2017 (Figure 1b), as the event lasted fewer than 15 days in March and May, preventing these months from being considered MHW months in this analysis. These two MHW events greatly exceed the average MHW duration (in days) in both regions: 16.2 ± 9.3 days in the MAB and 13.9 ± 7.8 in the SAB (Figure S1 in Supporting Information S1).

During the 2012 MAB event, SST anomalies exhibited a significant increase in the initial 3 months (February–April), followed by a gradual decline in May and June (Figure 2a). Therefore, we divided the 2012 MAB event into the early period from February to April 2012 and the later period from May to June 2012. During the early period, pCO_{2sea} anomalies experienced no significant difference, but a substantial surge of approximately 46 μatm above the climatology in May and remained notably positive until June (+36.9 ± 12.7 μatm) (Figure 2c). This increased pCO_2 impedes air-sea CO_2 exchange since the air-sea pCO_2 gradient becomes smaller (Equation 1). Additionally, the wind speed was -0.42 ± 0.34 m s^{-1} lower than the climatology throughout the entire event (Figure 2e), which also impedes the CO_2 uptake. Consequently, the average CO_2 flux anomaly is positive (+0.59 ± 0.55 mol C m^{-2} yr^{-1}), causing a 26% reduction of the MAB's average CO_2 uptake from the climatology (-2.31 ± 1.90 mol C m^{-2} yr^{-1}) during this event (Figure 2i). This uptake reduction is equivalent to 0.82 Tg C yr^{-1}, which reduces the MAB's 2012 annual net carbon uptake (in mol C yr^{-1}) by 13.7%.

Although it lasted only 44 days, the 2017 SAB event provides a valuable snapshot of CO_2 flux changes during MHW events in this region. Both SST and pCO_{2sea} exhibited positive anomalies before and after the MHW (Figure 2b). In April, however, both parameters showed a notable increase: the SST and pCO_{2sea} were +1.47°C and +99.2 μatm higher than climatology, respectively (Figures 2b and 2d). Thermodynamically, such a temperature increase alone accounted for a one-fourth rise in pCO_{2sea} of +25.3 μatm (Takahashi et al., 1993), while the non-thermal component contributed an additional +69.5 μatm. This highlights the significant amplification of the influence by non-thermal drivers during the 2017 SAB event, contrasting with the counteracting influence observed in the early period of the 2012 MAB event. Concurrently, wind speed slightly decreased (−0.35 m s^{-1}) in April. On average, climatological sea surface pCO_2 in the SAB tends to reach equilibrium with the atmosphere in April, with a flux of +0.10 ± 1.4 mol C m^{-2} yr^{-1}. However, during the 2017 event, the SAB transformed from CO_2 neutral into a significant CO_2 source with a flux anomaly of +2.07 mol C m^{-2} yr^{-1} (Figure 2j). This increased outgassing added an additional 2.66 Tg C yr^{-1} to the atmosphere, thereby reducing the SAB's 2017 annual carbon uptake (in mol C yr^{-1}) by 165%.

In both the 2012 and 2017 MHW events, flux anomaly was anomalously positive. Simultaneously, pCO_{2sea} was anomalously positive while wind speed was anomalously low. The first-order terms from the Taylor expansion of CO_2 flux during both the 2012 MAB and 2017 SAB events (Equation 11) reveal whether ΔpCO_2 (i.e., pCO_{2sea}) or wind speed (Γ in Figure S2 of the Supporting Information S1) was the primary driver of the flux anomaly during both events (Figure S2 in Supporting Information S1). A monthly breakdown of these contributions during the 2012 MAB event (Figure S2b in Supporting Information S1) shows that ΔpCO_2 was the primary contributor during 3 of the 5 months during the 2012 MAB event (i.e., February, May, and June), while wind speed dominated March and April. As such, ΔpCO_2 is generally considered the primary factor controlling FCO_2' during the entire 2012 MAB event. Similarly, ΔpCO_2 was the overwhelming contributor to FCO_2' during the 2017 SAB MHW event, with wind speed contributing inconsequently (Figures S2c and S2d in Supporting Information S1).

Understanding whether thermal (i.e., MHW) or non-thermal drivers of pCO_{2sea} were controlling pCO_{2sea} anomalies during each MHW event will determine whether the MHW or non-temperature factors were responsible for inducing the positive FCO_2' experienced during both case study events. During the 2012 MAB event, non-thermal drivers of pCO_{2sea} counteracted the thermal contribution from the MHW during the early period of the event but were unable to do so in the later period (Figure S3a in Supporting Information S1). Thus, processes controlling non-thermal pCO_{2sea} change in the MAB are potentially important buffers against MHW events because they can counteract either all or part of a MHW's thermal influence on FCO_2. During the 2017 SAB event, the MHW was not primarily responsible for the large magnitude of FCO_2' in April 2017 (Figure S3b in Supporting Information S1). Rather, non-thermal parameters dominated pCO_{2sea}' during the event. This highlights the increased importance of non-thermal drivers in the SAB compared with the MAB since the large magnitude of the non-thermal pCO_{2sea}' suggests these drivers may be capable of markedly amplifying or reducing MHW influences on pCO_{2sea}'.

With non-thermal pCO_{2sea} changes proving to be important in both regions, understanding the processes driving this parameter would be useful. However, without water-column total alkalinity and dissolved inorganic carbon data, a definitive answer regarding the mechanism(s) responsible for driving non-thermal pCO_{2sea} changes is beyond this study. However, work by Jones et al. (2014) on the CO_2 gas exchange timescale allows us to broadly hypothesize possible mechanisms. Assuming that open ocean timescales are the same in adjacent coastal regions, in the SAB region, the gas exchange timescale is longer than the mixed layer residence time. So, in this case, mixing processes are vital controls of pCO_{2sea} changes. In the MAB region, the opposite occurs; the gas exchange timescale is shorter than the mixed later residence time. Consequently, mixing is not a dominant control on gas exchange in this region. Instead, our results suggest that the timescale of thermally induced pCO_{2sea} changes resulting from MHWs in the MAB is shorter than that of air-sea gas exchange. This further highlights the importance of temperature as a dominant control in air-sea gas exchange in the MAB compared with non-thermal drivers. Non-thermal pCO_{2sea} changes in the MAB during the 2012 MHW event were likely biologically driven, as the bulk of the event occurred during the time period of the spring bloom (Cao et al., 2020; Signorini et al., 2013).

3.2. MHW Impacts on pCO_{2sea} Change

To assess whether the significant changes in pCO_{2sea} and CO_2 flux observed during the most prolonged events are representative of all MHW events, we statistically compared the pCO_{2sea} and flux anomalies between MHW and

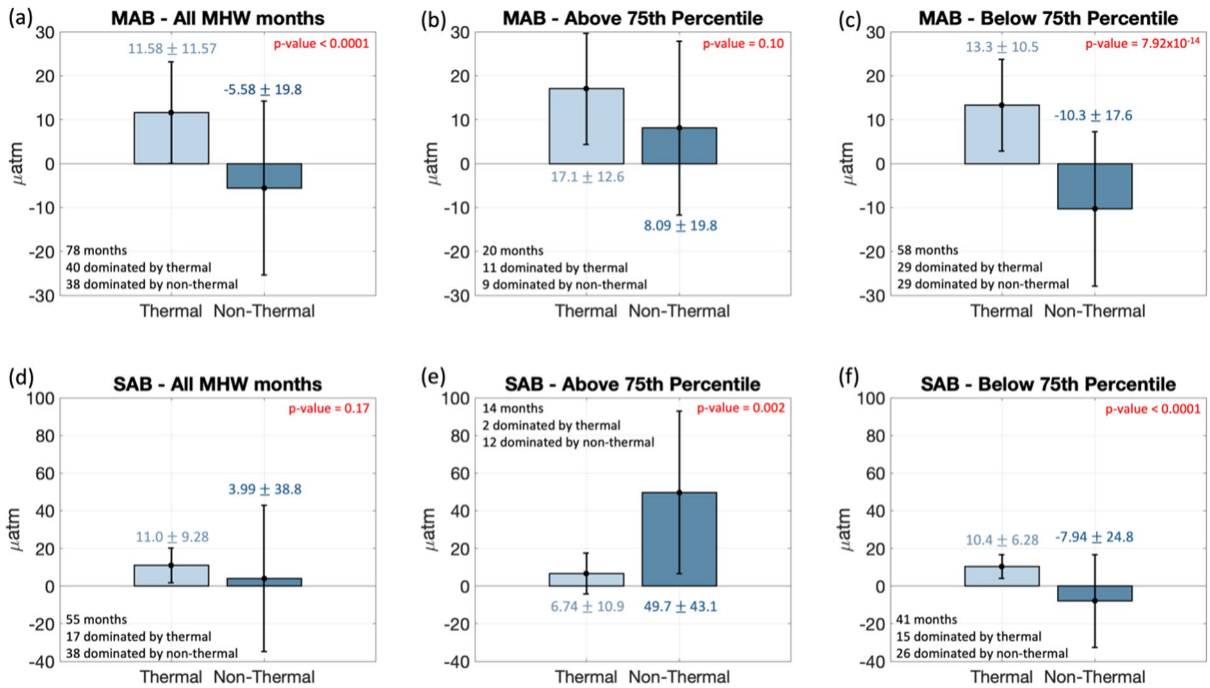

Figure 3. Mean and one standard deviation (error bars) of thermal (light blue bars) and non-thermal (dark blue bars) pCO_{2sea} anomalies in the (a through c) MAB and (d through f) SAB during MHW months with FCO_2 anomalies during (a and d) every MHW month and (b and e) above and (c and f) below the 75th percentile of CO_2 flux anomalies. *p*-values from a student's *t*-test are presented in red text, determining whether thermal and non-thermal components are statistically different from each other in each panel.

non-MHW months in the two regions. Over the 28-year study period (1992–2020), the ensemble mean flux anomalies during MHW months in the MAB and SAB ($+0.13 \pm 0.63$ and $+0.26 \pm 0.82$ mol C m^{-2} yr^{-1}, respectively) showed only slight differences compared to non-MHW months (-0.12 ± 0.81 and -0.14 ± 0.96 mol C m^{-2} yr^{-1}, respectively). While the ensemble mean flux anomaly during MHW months is statistically different from non-MHW months in both regions (*p*-values of 0.03 and 0.01 in the MAB and SAB, respectively), the large standard deviations indicate that a MHW alone is not a sufficient condition for the occurrence of positive flux anomalies. To identify conditions under which MHWs will associate with significant positive flux anomalies, we further divided MHW months into two categories: those above and below the 75th percentile FCO_2' values (+0.54 mol C m^{-2} yr^{-1} in the MAB and +0.84 mol C m^{-2} yr^{-1} in the SAB). This helps to distinguish whether MHWs or non-temperature factors are responsible for producing large, positive flux anomaly values, that is, those that fall above the 75th percentile. Both the 2012 and 2017 events fell above the 75th percentile threshold.

In the MAB, temperature exerts a more significant influence on pCO_{2sea} changes than other drivers during all MHW events (Figure 3a). Above the 75th percentile, both thermal and nonthermal drivers are important for producing a large positive flux anomaly (Figure 3b). Thermal contributions are usually larger than non-thermal influences, but the means of the two components are not statistically different (*p*-value = 0.10; Figure 3b). Nevertheless, temperature remains the primary contributor to pCO_{2sea} anomalies during these months, accounting for approximately 68% of the total pCO_{2sea} changes ($+17.1 \pm 12.6$ μatm). Like the early period of the 2012 MAB event, nonthermal drivers tend to counterbalance the impact of temperature on pCO_{2sea} during all MHW months (Figure 3a), especially in MHW months with flux anomalies below the 75th percentile (Figure 3c).

However, in MHW months above the 75th percentile in the MAB, nonthermal drivers amplify thermally induced positive pCO_{2sea} anomalies rather than offsetting the temperature's impact (Figure 3b). Furthermore, the importance of non-thermal processes as drivers of flux anomalies increases relative to the thermal component because, unlike MHW months below the 75th percentile, there is not a statistical difference between the two components during MHWs above the 75th percentile (Figure 3e). In general, MHWs produce a temperature-induced increase in pCO_{2sea} that is somewhat offset by non-temperature factors in the MAB. This is consistent with Mignot et al.'s (2022) result in the North Pacific subtropical gyre.

Version of Record at: https://doi.org/10.1029/2023GL105363

In the SAB, initial comparisons of all MHWs in this region (Figure 3d) to those in the MAB (Figure 3a) indicate that the magnitudes of thermally induced pCO_{2sea} changes in the SAB are similar to those in the MAB, with nonthermal drivers also playing a reduced role compared to MHWs. However, statistical analysis reveals that the thermal and non-thermal components in the SAB are not statistically different (p-value = 0.17), meaning non-thermal processes exert a greater influence in the SAB during MHW months (Figure 3d), as observed in the 2017 SAB event. Like the MAB, nonthermal drivers in months below the 75th percentile offset the impact of high temperatures (Figure 3f), resulting in pCO_{2sea} anomalies close to zero. However, for months above the 75th percentile (Figure 3e), the main contribution to pCO_{2sea} anomalies comes from nonthermal drivers (+49.7 ± 43.1 μatm) rather than extremely warm temperatures. This suggests that high pCO_{2sea} values during MHW events in the SAB are not solely caused by temperature itself, so it is inappropriate to conclude that MHW events have significant impacts on CO_2 flux in this region, unless the nonthermal drivers also produce a positive pCO_{2sea} during MHW events.

While MHWs appear to play a larger role driving air-sea gas exchange in the MAB, prolonged MHW events, like the 2012 MAB and 2017 SAB MHW events, can still produce a noticeable impact on interannual scales. The impact of these two events on the interannual variability of air-sea CO_2 flux anomalies is evident in Figure S4 of the Supporting Information S1. The years in which the two most prolonged MHWs occurred correspond to some of the highest annual flux anomalies over the 28-year study period. So, while non-thermal flux drivers are vital to produce large flux anomalies, especially in the SAB, prolonged MHWs are still a necessary condition to produce large changes in air-sea CO_2 flux.

3.3. Wind Speeds Change During All MHW Months

We also examined wind speed changes during MHW months since wind speed significantly impacts the magnitude of air-sea CO_2 flux (FCO_2), with faster winds generally resulting in higher gas transfer velocities (k) and larger FCO_2 values. Wind speeds were below the climatological average during the two most prolonged MHW events in the SAB and MAB. These slower wind speeds amplified MHW influences on FCO_2' by further decreasing the CO_2 sink in wintertime months but counteracting MHW effects in summertime months.

Reduced wind speeds were typical during many MHW months (Figure 4). Yet, like pCO_{2sea}, further investigation revealed that wind speeds did not significantly deviate from the climatology during all MHW events in the MAB and SAB (Figures 4a and 4d). However, among the 20 MHW months above the 75th percentile in the MAB (Figure 4b), 12 occurred during the wintertime when the MAB typically acts as a CO_2 sink. During these events, wind speeds were slower by −0.36 ± 0.50 m/s compared to the climatology, which may link to zonal shifts in the jet stream (Chen et al., 2014), significantly reducing the CO_2 sink in the MAB. In the SAB, wind speeds were generally slower than the climatological average during all MHW events (Figures 4d, 4e, and 4f). This indicates that wind speeds tend to decrease CO_2 uptake during CO_2-sink months but counteract the impact of MHWs on flux during CO_2-source months. However, the large standard deviations in wind speeds in both regions suggest that the effects of wind speed vary depending on the individual event.

3.4. Underlying Dynamics Between MHWs and CO_2 Flux on the US East Coast

During the 2012 MAB event, the extremely warm SSTs resulted in a significant increase in pCO_{2sea}, ultimately reducing the MAB's ability to take up CO_2. In contrast, despite the extremely high temperature during the 2017 SAB event, non-thermal drivers dominated the pCO_{2sea} increase. In April 2017, the increase in pCO_{2sea} was accompanied by a SSS change of −0.95 psu in the SAB, corresponding to a change in TA of −44.1 μmol kg^{-1} using the linear relationship (TA = 46.56 × SSS + 688.24) established by Xu et al. (2020). Given a climatological DIC value of 2015 μmol kg^{-1} (Xu et al., 2020), this reduction in TA would lead to a +73.8 μatm increase in pCO_{2sea}. This value is comparable to the non-thermal pCO_{2sea} increase of +69.5 μatm and accounts for 74.4% of the total pCO_{2sea} increase (+99.2 μatm) during the 2017 SAB event.

In the MAB, CO_2 flux into the ocean significantly decreased during MHW months, especially under weak-wind conditions in winter. This is particularly true for the atmospheric type of MHWs that were driven by anomalous air-sea heat flux, according to the classification of Oliver et al. (2021). In the case of atmospheric-type MHWs, perturbations in the atmosphere can lead to decreased wind speeds and downward

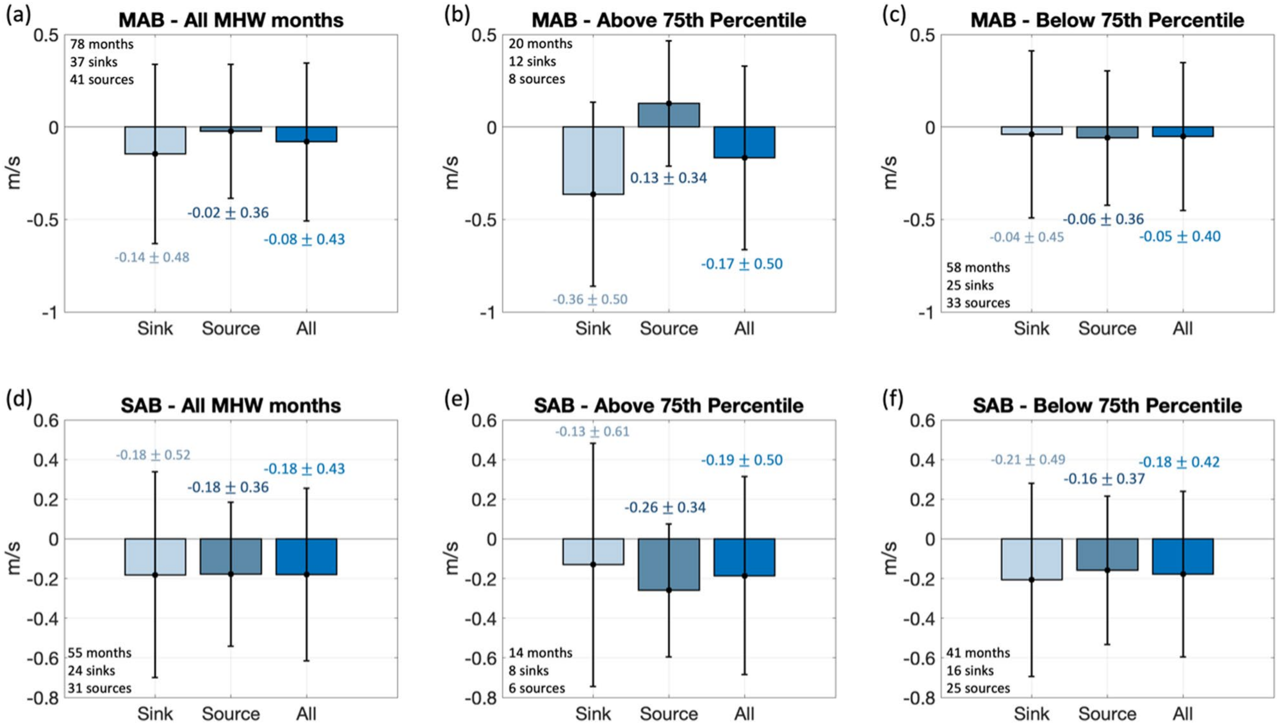

Figure 4. Wind speed anomalies during MHW months that are climatologically CO_2 sinks and sources during (a and d) all MHW months, (b and e) above the 75th percentile of flux anomalies, and (c and f) below the 75th percentile in the MAB (top panels) and SAB (bottom panels).

heat flux, both resulting in abnormally warm SST. These phenomena have been attributed to the zonal shift of the jet stream (Chen et al., 2014). Considering that winter MHW events above the 75th percentile also coincide with reduced wind speeds, it is plausible that this mechanism contributes to the occurrence of these MHW months. We, therefore, expanded upon the mechanism proposed by Chen et al. (2014) to explain how MHW events impact CO_2 flux in the MAB during winter months (Figure 5). In the MAB, the northward shift of the jet stream during winter causes a reduction in wind speeds, leading to a decrease in latent and sensible heat fluxes. This hinders heat loss from the ocean and results in a warmer sea surface that induces the MHW event. These elevated temperatures increase $p\mathrm{CO}_{2\mathrm{sea}}$, and the concurrence of weakened wind speeds further reduce CO_2 uptake by the ocean.

4. Summary and Conclusions

We investigated the impact of MHW events on air-sea CO_2 flux in the SAB and MAB over the past three decades. The sensitivity of the carbonate system to SST variability indicates that extreme temperatures during MHW events can influence carbon transfer between the atmosphere and the ocean. Interestingly, we found that while the two most prolonged MHW events in both regions resulted in large positive CO_2 flux anomalies (FCO_2'), MHWs alone were insufficient to guarantee positive flux anomalies. By analyzing MHW months that exceeded the 75th percentile of CO_2 flux anomalies, we identified specific conditions that lead to substantial flux changes. In the SAB, MHWs were not directly responsible for flux changes, and $p\mathrm{CO}_{2\mathrm{sea}}$ variations during MHW events were attributed to factors other than temperature. In contrast, MHWs played a more significant role in the MAB, though non-thermal drivers were still vital to produce significant positive $p\mathrm{CO}_{2\mathrm{sea}}$ changes. The prevalence of reduced wind speeds during MHW months above the 75th percentile in the MAB led us to append the influence of MHWs on $p\mathrm{CO}_{2\mathrm{sea}}$ to Chen et al.'s (2014) mechanism for wintertime air-sea heat flux MHW induction. We add that the northward shift of the wintertime jet stream in the MAB results in weakened wind speeds and downward heat flux, leading to increased SST and, thus, $p\mathrm{CO}_{2\mathrm{sea}}$. This combination of factors further reduced the ocean's ability to uptake CO_2.

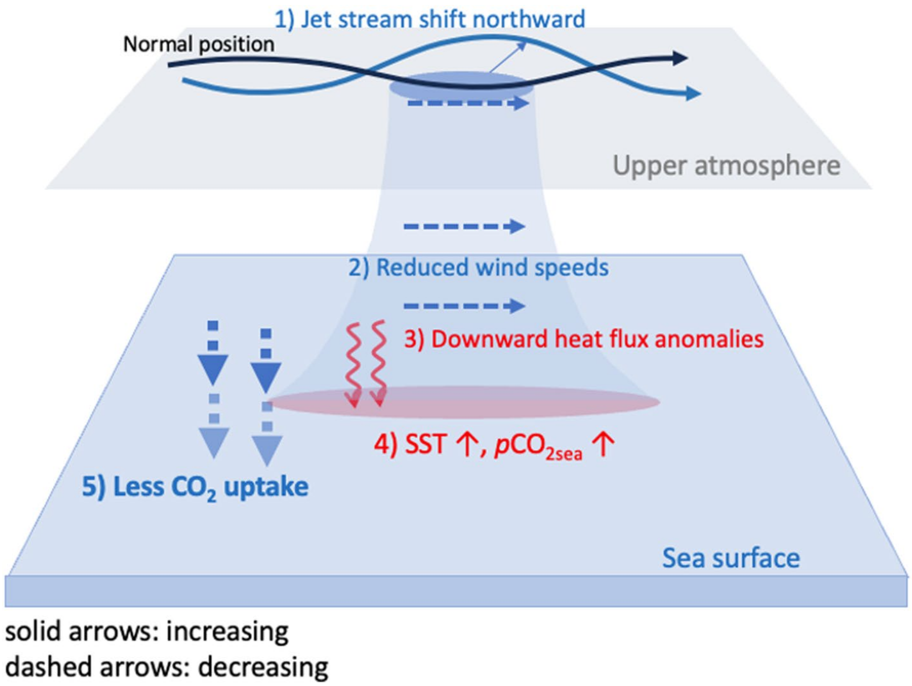

Figure 5. Conceptual diagram of mechanisms connecting MHWs and CO_2 flux in the MAB. The solid arrows indicate increasing vectors or fluxes, and the dashed arrows represent decreasing vectors. The numbers represent the order of occurrence for the respective processes.

Data Availability Statement

The SOCAT data used in the analysis are available at https://socat.info/index.php/data-access/. The NOAA OISST v2 data used for analysis are available at https://psl.noaa.gov/data/gridded/data.noaa.oisst.v2.high-res.html. NOAA's Greenhouse Gas Marine Boundary Layer Reference used for analysis are available at https://gml.noaa.gov/ccgg/mbl/data.php. ERA5 wind magnitudes used for analysis are available at https://cds.climate.copernicus.eu/cdsapp#!/dataset/reanalysis-era5-single-levels-monthly-means?tab=overview.

Acknowledgments

Zelun Wu acknowledges support from the National Natural Science Foundation of China (91858202) and the Ph.D. Fellowship of the State Key Laboratory of Marine and Environment Science at Xiamen University. Kelsea Edwing and Xiao-Hai Yan acknowledge support from the National Science Foundation (NSF-IIS-2123264), and the National Aeronautics and Space Administration (NASA-80NSSC20M0220). Wei-Jun Cai acknowledges support from the NOAA's Ocean Acidification Program (OAP) on data collection and synthesis. Kelsea Edwing analyzed data and wrote the paper. Zelun Wu conceived the idea, helped with the discussion, and revised the manuscript. Dr. Xinyu Li, Dr. Wenfang Lu, Dr. Wei-Jun Cai, and Dr. Xiao-Hai Yan revised the manuscript. All authors contributed to the discussion and improvement of the work. We thank NOAA, the Remote Sensing System, and the carbonate community (SOCAT) for sharing their data.

References

Cahill, B., Wilkin, J., Fennel, K., Vandemark, D., & Friedrichs, M. A. M. (2016). Interannual and seasonal variabilities in air-sea CO_2 fluxes along the U.S. eastern continental shelf and their sensitivity to increasing air temperatures and variable winds. *Journal of Geophysical Research: Biogeosciences*, *121*(2), 295–311. https://doi.org/10.1002/2015JG002939

Cai, W.-J., Xu, Y.-Y., Feely, R. A., Wanninkhof, R., Jönsson, B., Alin, S. R., et al. (2020). Controls on surface water carbonate chemistry along North American ocean margins. *Nature Communications*, *11*(1), 2691. Article 1. https://doi.org/10.1038/s41467-020-16530-z

Cao, Z., Yang, W., Zhao, Y., Guo, X., Yin, Z., Du, C., et al. (2020). Diagnosis of CO_2 dynamics and fluxes in global coastal oceans. *National Science Review*, *7*(4), 786–797. https://doi.org/10.1093/nsr/nwz105

Chen, K., Gawarkiewicz, G., Kwon, Y.-O., & Zhang, W. G. (2015). The role of atmospheric forcing versus ocean advection during the extreme warming of the Northeast U.S. continental shelf in 2012. *Journal of Geophysical Research: Oceans*, *120*(6), 4324–4339. https://doi.org/10.1002/2014JC010547

Chen, K., Gawarkiewicz, G. G., Lentz, S. J., & Bane, J. M. (2014). Diagnosing the warming of the Northeastern U.S. Coastal Ocean in 2012: A linkage between the atmospheric jet stream variability and ocean response. *Journal of Geophysical Research: Oceans*, *119*(1), 218–227. https://doi.org/10.1002/2013JC009393

Conway, T. J., Tans, P. P., Waterman, L. S., Thoning, K. W., Kitzis, D., Masarie, K. A., & Zhang, N. (1994). Evidence for interannual variability of the carbon cycle from the national oceanic and atmospheric administration/climate monitoring and diagnostics laboratory global air sampling network. *Journal of Geophysical Research*, *99*(D11), 22831–22855. JD01951. https://doi.org/10.1029/94jd01951

Dai, M., Su, J., Zhao, Y., Hofmann, E., Cao, Z., Cai, W.-J., et al. (2022). Carbon fluxes in the coastal ocean: Synthesis, boundary processes, and future trends. *Annual Review of Earth and Planetary Sciences*, *50*(1), 593–626. https://doi.org/10.1146/annurev-earth-032320-090746

DeGrandpre, M. D., Olbu, G. J., Beatty, C. M., & Hammar, T. R. (2002). Air–sea CO_2 fluxes on the US Middle Atlantic Bight. *Deep Sea Research Part II: Topical Studies in Oceanography*, *49*(20), 4355–4367. https://doi.org/10.1016/S0967-0645(02)00122-4

Dye, S., Hughes, S., Tinker, J., Berry, D., Holliday, N., & Kent, E. (2013). Impacts of climate change on temperature (air and sea). *Marine Climate Change Impacts Partnership: Science Review*, 1–12.

Elsner, J. (2006). Evidence in support of the climate change–Atlantic hurricane hypothesis. *Geophysical Research Letters*, *33*(16), L16705. https://doi.org/10.1029/2006GL026869

Fennel, K., Wilkin, J., Previdi, M., & Najjar, R. (2008). Denitrification effects on air-sea CO_2 flux in the coastal ocean: Simulations for the northwest North Atlantic. *Geophysical Research Letters*, *35*(24), L24608. https://doi.org/10.1029/2008GL036147

Friedlingstein, P., O'Sullivan, M., Jones, M. W., Andrew, R. M., Gregor, L., Hauck, J., et al. (2022). Global carbon budget 2022. *Earth System Science Data*, *14*(11), 4811–4900. https://doi.org/10.5194/essd-14-4811-2022

Frölicher, T. L., Fischer, E. M., & Gruber, N. (2018). Marine heatwaves under global warming. *Nature*, *560*(7718), 360–364. https://doi.org/10.1038/s41586-018-0383-9

Gattuso, J.-P., Frankignoulle, M., & Wollast, R. (1998). Carbon and carbonate metabolism in coastal aquatic ecosystems. *Annual Review of Ecology and Systematics*, *29*(1), 405–434. https://doi.org/10.1146/annurev.ecolsys.29.1.405

Gawarkiewicz, G., Chen, K., Forsyth, J., Bahr, F., Mercer, A. M., Ellertson, A., et al. (2019). Characteristics of an advective marine heatwave in the Middle Atlantic Bight in early 2017. *Frontiers in Marine Science*, *6*, 712. https://doi.org/10.3389/fmars.2019.00712

Hersbach, H., Bell, B., Berrisford, P., Biavati, G., Horányi, A., Muñoz Sabater, J., et al. (2023). ERA5 hourly data on single levels from 1940 to present. *Copernicus Climate Change Service (C3S) Climate Data Store (CDS)*. https://doi.org/10.24381/cds.adbb2d47

Hobday, A. J., Alexander, L. V., Perkins, S. E., Smale, D. A., Straub, S. C., Oliver, E. C. J., et al. (2016). A hierarchical approach to defining marine heatwaves. *Progress in Oceanography*, *141*, 227–238. https://doi.org/10.1016/j.pocean.2015.12.014

Hobday, A. J., Oliver, E. C. J., Gupta, A. S., Benthuysen, J. A., Burrows, M. T., Donat, M. G., et al. (2018). Categorizing and naming marine heatwaves. *Oceanography*, *31*(2), 162–173. https://doi.org/10.5670/oceanog.2018.205

Jentsch, A., Kreyling, J., & Beierkuhnlein, C. (2007). A new generation of climate-change experiments: Events, not trends. *Frontiers in Ecology and the Environment*, *5*(7), 365–374. https://doi.org/10.1890/1540-9295(2007)5[365:ANGOCE]2.0.CO;2

Jiang, L.-Q., Cai, W.-J., Wang, Y., & Bauer, J. E. (2013). Influence of terrestrial inputs on continental shelf carbon dioxide. *Biogeosciences*, *10*(2), 839–849. https://doi.org/10.5194/bg-10-839-2013

Jiang, L.-Q., Cai, W.-J., Wanninkhof, R., Wang, Y., & Lüger, H. (2008). Air-sea CO_2 fluxes on the U.S. South Atlantic Bight: Spatial and seasonal variability. *Journal of Geophysical Research*, *113*(C7), C07019. https://doi.org/10.1029/2007JC004366

Jones, D. C., Ito, T., Takano, Y., & Hsu, W.-C. (2014). Spatial and seasonal variability of the air-sea equilibration timescale of carbon dioxide. *Global Biogeochemical Cycles*, *28*(11), 1163–1178. https://doi.org/10.1002/2014GB004813

Large, W. G., & Yeaher, S. G. (2012). *On the observed trends and changes in global sea surface temperature and air–sea heat fluxes (1984–2006)* (pp. 6123–6135). American Meteorological Society. https://doi.org/10.1175/JCLI-D-11-00148.1

Laruelle, G. G., Cai, W.-J., Hu, X., Gruber, N., Mackenzie, F. T., & Regnier, P. (2018). Continental shelves as a variable but increasing global sink for atmospheric carbon dioxide. *Nature Communications*, *9*(1), 454. Article 1. https://doi.org/10.1038/s41467-017-02738-z

Le Quéré, C., Raupach, M., Canadell, J., Marland, G., Bopp, L., Ciais, P., et al. (2009). Trends in the sources and sinks of carbon dioxide. *Nature Geoscience*, *2*(12), 831–836. https://doi.org/10.1038/ngeo689

Le Quéré, C., Takahashi, T., Buitenhuis, E. T., Rödenbeck, C., & Sutherland, S. C. (2010). Impact of climate change and variability on the global oceanic sink of CO_2. *Global Biogeochemical Cycles*, *24*(4). https://doi.org/10.1029/2009GB003599

Li, X., Xu, Y.-Y., Kirchman, D. L., & Cai, W.-J. (2022). Carbonate parameter estimation and its application in revealing temporal and spatial variation in the South and Mid-Atlantic Bight, USA. *Journal of Geophysical Research: Oceans*, *127*(7), e2022JC018811. https://doi.org/10.1029/2022JC018811

Liu, K.-K., Atkinson, L., Quiñones, R., & Talaue-McManus, L. (2010). *Carbon and nutrient fluxes in continental margins: A global synthesis*. Springer Science & Business Media.

Mignot, A., Schuckmann, K. V., Gasparin, F., van Gennip, S., Landschützer, P., Perruche, C., et al. (2022). Decrease in air-sea CO_2 fluxes caused by persistent marine heatwaves. Retrieved from https://eartharxiv.org/repository/view/1993/

R. G. Najjar, M. A. M. Friedrichs, & W.-J. Cai (Eds.) (2012). *Report of the U.S. East Coast carbon cycle synthesis workshop, January 19-20, 2012* (p. 34). Ocean Carbon and Biogeochemistry Program and North American Carbon Program.

Oliver, E. C. J., Benthuysen, J. A., Darmaraki, S., Donat, M. G., Hobday, A. J., Holbrook, N. J., et al. (2021). Marine heatwaves. *Annual Review of Marine Science*, *13*(1), 313–342. https://doi.org/10.1146/annurev-marine-032720-095144

Oliver, E. C. J., Donat, M. G., Burrows, M. T., Moore, P. J., Smale, D. A., Alexander, L. V., et al. (2018). Longer and more frequent marine heatwaves over the past century. *Nature Communications*, *9*(1), 1324. https://doi.org/10.1038/s41467-018-03732-9

Reynolds, R. W., Rayner, N. A., Smith, T. M., Stokes, D. C., & Wang, W. (2002). An improved in situ and satellite SST analysis for climate. *Journal of Climate*, *15*(13), 1609–1625. https://doi.org/10.1175/1520-0442(2002)015<1609:aiisas>2.0.co;2

M. J. Salinger, M. V. K. Siva Kumar, & R. P. Motha (Eds.) (2005). *Increasing climate variability and change: Reducing the vulnerability of agriculture and forestry*. Springer.

Sarmiento, J., & Gruber, N. (2006). *Ocean biogeochemical dynamics* (pp. 318–340). Princeton University Press.

Scannell, H. A., Pershing, A. J., Alexander, M. A., Thomas, A. C., & Mills, K. E. (2016). Frequency of marine heatwaves in the North Atlantic and North Pacific since 1950. *Geophysical Research Letters*, *43*(5), 2069–2076. https://doi.org/10.1002/2015GL067308

Seager, R., Cane, M., Henderson, N., Lee, D. E., Abernathey, R., & Zhang, H. (2019). Strengthening tropical Pacific zonal sea surface temperature gradient consistent with rising greenhouse gases. *Nature Climate Change*, *9*(7), 517–522. https://doi.org/10.1038/s41558-019-0505-x

Signorini, S. R., Mannino, A., Najjar, R. G., Jr., Friedrichs, M. A. M., Cai, W.-J., Salisbury, J., et al. (2013). Surface ocean pCO_2 seasonality and sea-air CO_2 flux estimates for the North American east coast. *Journal of Geophysical Research: Oceans*, *118*(10), 5439–5460. https://doi.org/10.1002/jgrc.20369

Sillmann, J., & Roeckner, E. (2007). Indices for extreme events in projections of anthropogenic climate change. *Climate Change*, *86*(1–2), 83–104. https://doi.org/10.1007/s10584-007-9308-6

Stott, P. (2016). How climate change affects extreme weather events. *Science*, *352*(6923), 1517–1518. https://doi.org/10.1126/science.aaf7271

Takahashi, T., Olafsson, J., Goddard, J. G., Chipman, D. W., & Sutherland, S. C. (1993). Seasonal variation of CO_2 and nutrients in the high-latitude surface oceans: A comparative study. *Global Biogeochemical Cycles*, *7*(4), 843–878. https://doi.org/10.1029/93GB02263

Takahashi, T., Sutherland, S., Sweeney, C., Poisson, A., Metzl, N., Tilbrook, B., et al. (2002). Global sea-sir CO_2 flux based on climatological surface ocean pCO_2, and seasonal biological and temperature effects. *Deep Sea Research Part II: Topical Studies in Oceanography*, *49*(9–10), 1601–1622. https://doi.org/10.1016/S0967-0645(02)00003-6

Takahashi, T., Sutherland, S. C., & Kozyr, A. (2019). Global ocean surface water partial pressure of CO_2 database: Measurements performed during 1957–2018 (LDEO database version 2018) (NCEI Accession 0160492). Version 7.7. *NOAA National Centers for Environmental Information*. Retrieved from https://www.nodc.noaa.gov/archive/arc0105/0160492/7.7/data/0-data/

Wanninkhof, R. (2014). Relationship between wind speed and gas exchange over the ocean revisited: Gas exchange and wind speed over the ocean. *Limnology and Oceanography: Methods*, *12*(6), 351–362. https://doi.org/10.4319/lom.2014.12.351

Wanninkhof, R., Asher, W., Ho, D., Sweeney, C., & McGillis, W. (2009). Advances in quantifying air-sea gas exchange and environmental forcing. *Annual Review of Marine Science*, *1*, 213–244. https://doi.org/10.1146/annurev.marine.010908.163742

Wanninkhof, R., & Triñanes, J. (2017). The impact of changing wind speeds on gas transfer and its effect on global air-sea CO_2 fluxes. *Global Biogeochemical Cycles*, *31*(6), 961–974. https://doi.org/10.1002/2016GB005592

Weiss, R. F. (1974). Carbon dioxide in water and seawater: The solubility of a non-ideal gas. *Marine Chemistry*, *2*(3), 203–215. https://doi.org/10.1016/0304-4203(74)90015-2

Weiss, R. F., & Price, B. A. (1980). Nitrous oxide solubility in water and seawater. *Marine Chemistry*, *8*(4), 347–359. https://doi.org/10.1016/0304-4203(80)90024-9

Xu, Y.-Y., Cai, W.-J., Wanninkhof, R., Salisbury, J., Reimer, J., & Chen, B. (2020). Long-term changes of carbonate chemistry variables along the North American east coast. *Journal of Geophysical Research: Oceans*, *125*(7), e2019JC015982. https://doi.org/10.1029/2019JC015982